Light Meson Decays from Photon-Induced Reactions with CLAS

Michael C. Kunkel[1,a)] and for the CLAS Collaboration

[1]*Forschungszentrum Jülich, Jülich (Germany)*

[a)]m.kunkel@fz-juelich.de

Abstract. Photoproduction of the π^0 meson was studied using the CLAS detector at Thomas Jefferson National Accelerator Facility using tagged incident beam energies spanning the range E_γ = 1.1 GeV - 5.45 GeV. The measurement is performed on a liquid hydrogen target in the reaction $\gamma p \rightarrow pe^+e^-(\gamma)$. The final state of the reaction is the sum of two subprocesses for π^0 decay, the Dalitz decay mode of $\pi^0 \rightarrow e^+e^-\gamma$ and conversion mode where one photon from $\pi^0 \rightarrow \gamma\gamma$ decay is converted into a e^+e^- pair. This specific final state reaction avoided limitations caused by single prompt track triggering and allowed a kinematic range extension to the world data on π^0 photoproduction to a domain never systematically measured before.

We report the measurement of the π^0 differential cross-sections $\frac{d\sigma}{d\Omega}$ and $\frac{d\sigma}{dt}$. The angular distributions agree well with the SAID parametrization for incident beam energies below 3 GeV, while an interpretation of the data for incident beam energies greater than 3 GeV is currently being developed. Included in the report will be a discussion of the future wide angle, exclusive photoproduction of π^0 experiment that will be performed in Hall C.

INTRODUCTION

In hadron physics, photoproduction of single pion is essential to understand the photon-nucleon vertex. At low energies, the photon-nucleon coupling establishes excited nucleon resonances which has been at the forefront of physics "missing resonances" search. At high energies single pion photoproduction can be used to test predictions of Regge theory, in which recent calculations [1] have shown to describe the presented data well. Furthermore, these measurements have shown that the differential cross section for single pion photoproduction at fixed c.m. angles, $\theta_{c.m.}$, of 70°, 90°and110° seem to scale as $\frac{d\sigma}{dt} \sim s^{2-n} f(\theta_{c.m.})$, where s and t are the Mandelstam variables and n is the total number of interacting elementary fields in the initial and final state of the reaction. This is predicted by the constituent counting rule [2, 3] and exclusive measurements in pp and $\bar{p}p$ elastic scattering [4, 5], meson-baryon Mp reactions [5], and photoproduction γN [6, 7, 8, 9, 10, 11, 12, 13] agree well with this rule . The following proceeding detailed the CLAS g12 experiment, the extraction of single neutral pion photoproduction from data, the differential cross-sections through the entire beam energy range of the g12 experiment, a comparison of the differential cross-section with existing world data, as well as the comparison of the data to the model given in [1], comparison to the constituent counting rule. Also presented will be an overview of a future measurement to be taken at Hall C to extended the measurement of neutral pion photoproduction at higher photon energies.

CLAS

The CLAS detector, shown in Fig. 1, is assembled of four types of detectors, five detectors total, that are arranged in an onion like pattern (around the beam line) covering $\sim 3\pi$ with a diameter of 8 m. Each layer is segmented such that there are six segments around ϕ (angle about the beam line), called sectors, each with a polar coverage, θ (angle from beam line), of approximately $\frac{3}{4}\pi$ radians. Each sector consists of a scintillator start counter (ST), three layers of drift chambers (DC), a layer of scintillator "time-of-flight" counters (TOF), a gas Cherenkov counter (CC) and an electromagnetic calorimeter (EC). There is a toroidal magnetic field generated by six superconducting coils that divide the sectors. The direction of the toroidal field is azimuthal, ϕ (angle about the beam line), such that the charged

particles conserve their azimuthal angle along their trajectory, except near the coils. The magnetic field geometry guides the particles which allows for a simplified reconstruction algorithm to determine the particles' momenta.

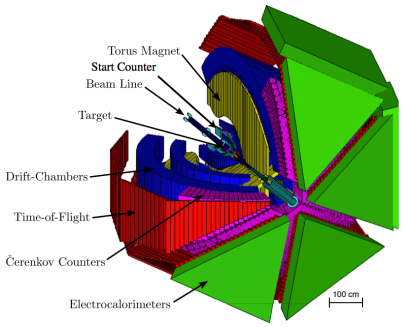

FIGURE 1: The CEBAF Large Acceptance Spectrometer (CLAS)

The g12 Experiment

The *g12* experiment is a photoproduction experiment, it ran during March - June 2008 with a total of 44 days of good beam time. It collected over 128 TB of raw data that consisted of $26 \cdot 10^9$ events, with an integrated luminosity of 68 pb^{-1}. The photon beam was produced by impinging a 5.715 GeV electron beam, at 65nA, on a Au radiator of 10^{-4} radiation length. Photons in the energy range from 20% to 95% of the electron beam energy were tagged, resulting in a photon beam energy range of 1.1-5.5 GeV. This photon beam was then collimated before being introduced onto a ℓH_2 target 40 cm in length along the z-direction and 2 cm radius. The placement of the target was 90 cm upstream from CLAS center (toward Au radiator), this increased the acceptance of particles in the forward direction. During the runtime of *g12*, the Cherenkov detectors were filled with perfluorobutane (C_4F_{10}) allowing for electron/positron detection. The experiment had a dedicated trigger, amongst 9 other triggers, that consisted of CC and EC coincidence hits for the entire beam energy range. With proper cuts on the CC and EC a π/e rejection of 10^6 for $e^{\pm}$ pairs was established.

Particle Selection

Particle selection consisted of all beam photons that were within 1.002 ns timing coincidence of the event, 1 proton and 2 oppositely charged tracks that were not the proton. This selection is appropriate for identifying the $\pi^0 \to e^+e^-\gamma$ decay because the mass of the π^0 is less than that of $\pi^{\pm}$, meaning π^0 cannot decay into $\pi^+\pi^-$.

Kinematic Cuts

Comparison to Existing Data

Comparison to Regge Model

s^7 Scaling

HALL C at Jlab12 Outlook

REFERENCES

[1] V. Mathieu *et al.*, Phys. Rev. **D92**, p. 074013 (2015), arXiv:1505.02321 [hep-ph] .
[2] S. J. Brodsky and G. R. Farrar, Phys. Rev. Lett. **31**, 1153–1156 (1973).
[3] G. P. Lepage and S. J. Brodsky, Phys. Rev. D **22**, 2157–2198 (1980).
[4] P. Landshoff and J. Polkinghorne, Physics Letters B **44**, 293 – 295 (1973).

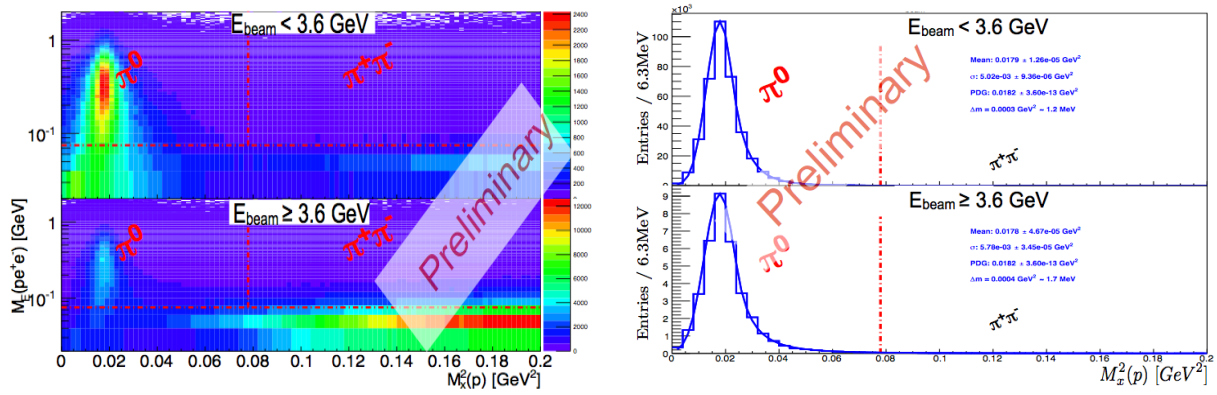

FIGURE 2: Left: $M_x^2(p)$ vs. $M_E(pe^+e^-)$. The horizontal red dashed-dotted line depicts the 75 MeV cut used in this analysis. The vertical red dashed-dotted line depicts the boundary of single π^0 to $\pi^+\pi^-$ production. Right: Final $M_x^2(p)$ data used in analysis. The horizontal red dashed-dotted line depicts the threshold of $\pi^+\pi^-$ production.

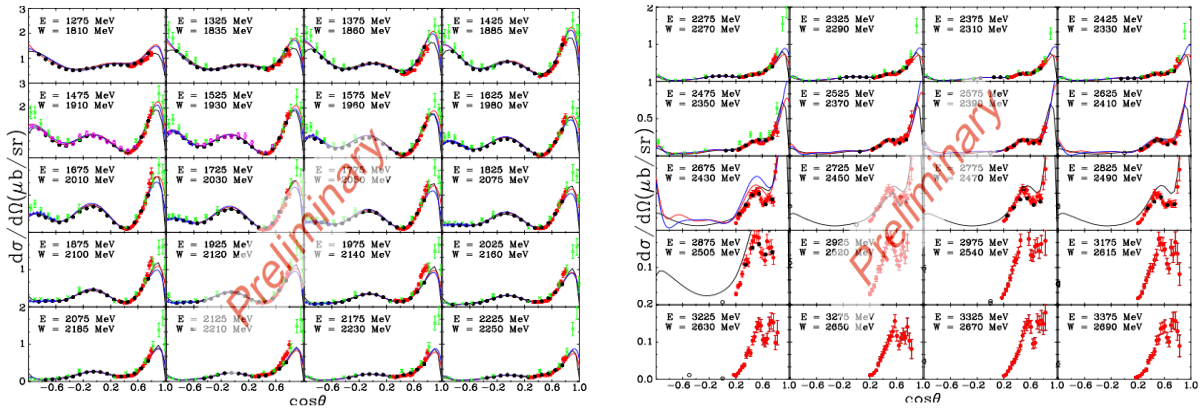

FIGURE 3: Left: $M_x^2(p)$ vs. $M_E(pe^+e^-)$. The horizontal red dashed-dotted line depicts the 75 MeV cut used in this analysis. The vertical red dashed-dotted line depicts the boundary of single π^0 to $\pi^+\pi^-$ production. Right: Final $M_x^2(p)$ data used in analysis. The horizontal red dashed-dotted line depicts the threshold of $\pi^+\pi^-$ production.

[5] R. L. Anderson *et al.*, Phys. Rev. D **49** (1994).
[6] W. Chen *et al.* (The CLAS Collaboration), Phys. Rev. Lett. **103**, p. 012301 (2009).
[7] L. Y. Zhu *et al.* (Jefferson Lab Hall A Collaboration), Phys. Rev. Lett. **91**, p. 022003 (2003).
[8] R. A. Schumacher and M. M. Sargsian, Phys. Rev. C **83** (2011).
[9] R. L. Anderson *et al.*, Phys. Rev. D **14**, 679–697 (1976).
[10] J. Napolitano *et al.*, Phys. Rev. Lett. **61**, 2530–2533 (1988).
[11] J. E. Belz *et al.*, Phys. Rev. Lett. **74**, 646–649 (1995).
[12] C. Bochna *et al.*, Phys. Rev. Lett. **81**, 4576–4579 (1998).
[13] E. C. Schulte and others., Phys. Rev. Lett. **87** (2001).

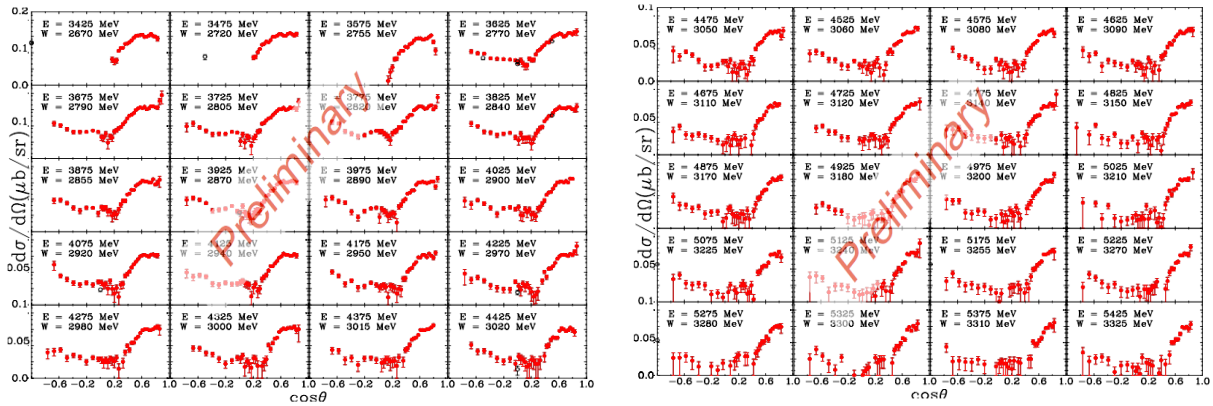

FIGURE 4: Left: $M_x^2(p)$ vs. $M_E(pe^+e^-)$. The horizontal red dashed-dotted line depicts the 75 MeV cut used in this analysis. The vertical red dashed-dotted line depicts the boundary of single π^0 to $\pi^+\pi^-$ production. Right: Final $M_x^2(p)$ data used in analysis. The horizontal red dashed-dotted line depicts the threshold of $\pi^+\pi^-$ production.

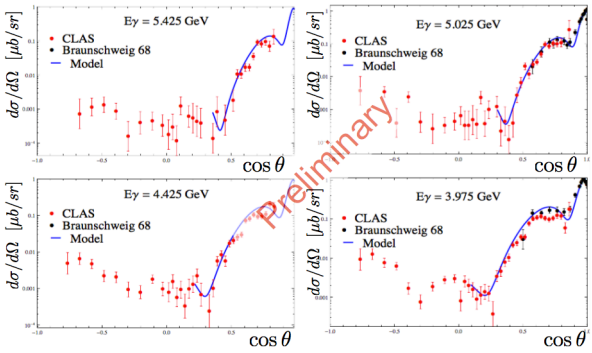

FIGURE 5: Comparison with Regge model. Caption embedded.

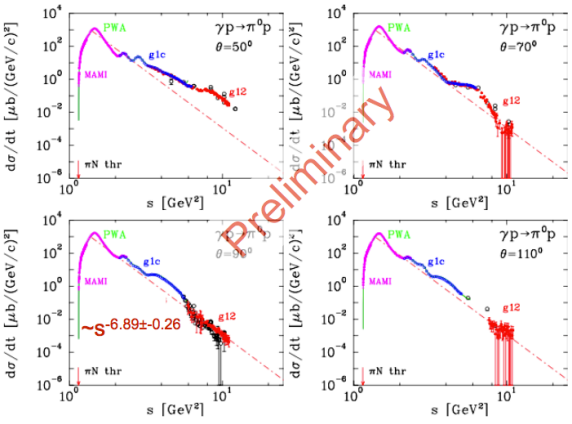

FIGURE 6: Comparison with scaling rule.

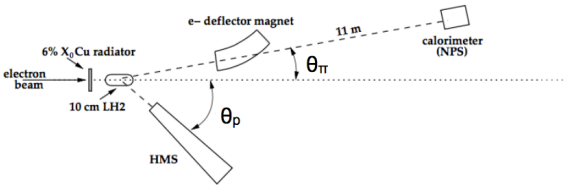

FIGURE 7: Comparison with scaling rule.

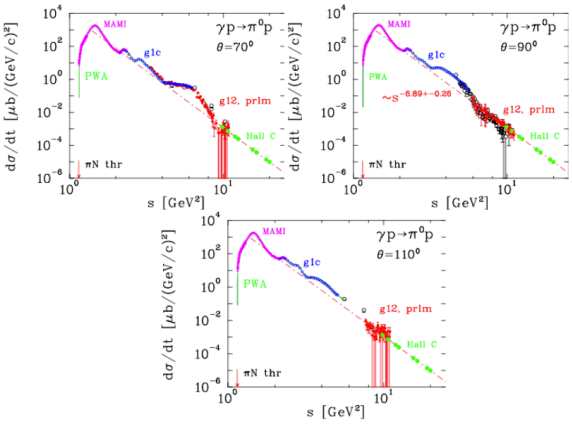

FIGURE 8: Comparison with scaling rule.